



Removal of fluoride from well water by modified iron oxides in a column system

J.J. García-Sánchez^{a,c}, M. Solache-Ríos^{a,*}, M.T. Alarcón-Herrera^d, V. Martínez-Miranda^b

^aDepto. de Química, Instituto Nacional de Investigaciones Nucleares, Apdo. Postal 18-1027, 11801 Mexico, D.F, Mexico, Tel. +52 5553297200, ext. 2271; Fax: +52 5553297301; emails: josejuangarcia1970@yahoo.com.mx (J.J. García-Sánchez), marcos.solache@inin.gob.mx (M. Solache-Ríos)

^bFacultad de Ingeniería, Centro Interamericano de Recursos del Agua, Universidad Autónoma del Estado de México, km. 14.5, Carretera Toluca-Ixtlahuaca, Toluca, Estado de México, Mexico, email: mmirandav@uaemex.mx

^cFacultad de Química, Universidad Autónoma del Estado de México, Paseo Colón y Tollocan s/n., C.P. 50000 Toluca, Estado de México, Mexico

^dCentro de Investigación en Materiales Avanzados (CIMAV), Ave. Miguel de Cervantes 120, Complejo Industrial Chihuahua, C.P. 31109 Chihuahua, Chih., Mexico, email: teresa.alarcon@cimav.edu.mx

Received 26 June 2014; Accepted 16 October 2014

ABSTRACT

The removal of fluoride from water by aluminum modified iron oxides (CP-Al) using a fixed-bed column adsorption system was investigated. Fixed-bed column experiments were carried out at different bed depths, and flow rate of 2 mL/min. The Bohart–Adams model and the Thomas model were applied to the experimental results. The adsorption efficiency decreases as the bed depth increases. The adsorption capacity for fluoride ions by CP-Al is higher for fluoride aqueous solutions than well water. The regeneration was accomplished by eluting a 0.1 M NaOH through the fluoride-loaded CP-Al bed. Scale-up and kinetic approach methods were used to calculate the design parameters from the breakthrough curves of fixed-bed column experiments. The parameters calculated from both methods indicated that they were suitable for fixed-bed column design.

Keywords: Fluoride; Corrosion products; Aluminum; Adsorption; Well water

1. Introduction

Fluoride occurs naturally in some waters, but it is frequently added to municipal water supplies because of a widely held belief that it prevents dental decay, although this additional concentration is very expensive and little usable. Fluoride levels in drinking and cooking water sources are strongly correlated with fluorosis severity [1].

Several methods have been applied to remove excessive fluoride from aqueous solution, such as adsorption [2,3], ion-exchange [4], precipitation [5], reverse osmosis [6], and electrodialysis [7]. Among these methods, adsorption is still one of the most extensively used methods because of its simplicity and the availability of a wide range of adsorbents. In recent years, much effort has been devoted to the investigation and development of new and cost-effective fluoride sorbents using various materials such as activated alumina [2], bleaching earth [8], rare earth

*Corresponding author.

oxides [9], clay [10], soil [11], bone char [12], zeolites [13], granular ferric hydroxide [14], and biosorbent [15].

The adsorption is the most widely used process for excess fluoride removal from aqueous solution, especially at the fluoride endemic areas of the developing countries. In this process, a packed bed of adsorbent in fixed columns is continuously used for cyclic sorption and/or desorption of pollutants by effectively utilizing the capacity of an adsorbent bed. From a relatively bulk liquid volume, the pollutant gets concentrated and confined onto a small adsorbent mass which can invariably be regenerated, reused, or safely disposed under control [16]. Since the nature and characteristics of water to be treated, and the presence of co-existing ions are decisive factors in sorption, the adsorption capacity derived from column studies of natural ground water would be a most reliable indicator for its field use. The objective of this paper was to determine the adsorption behavior of fluoride ions by aluminum modified iron oxides in a column system and compares two methods to scale-up the adsorption system and evaluate the effect of the anions and cations on the adsorption of fluoride.

2. Materials and methods

2.1. Materials and solutions

Corrosion products (CP) were obtained and modified as reported in a previous work [17], the oxides were crushed and sieved between 50 and 100 meshes (0.297 and 0.149 mm). A solution of 3 mg/L of fluoride ions (pH 6.5) was prepared from a standard sodium fluoride solution of 100 mg/L, and well water containing naturally 2.8 mg F⁻/L of pH 8.1 was used for the experiments.

2.2. Fluoride measurements

The fluoride concentrations in the remaining solutions were measured with a specific ion electrode (ISE301F) by using total ionic strength adjustment buffer solution to eliminate the interference of complexing ions.

2.3. Zeta potential measurements

Electrophoretic mobility measurements were conducted using a zeta meter model 3.0+ (Zeta Meter Inc., USA). The instrument determines the electrophoretic mobility of the particles automatically and converts it to the zeta (ζ) potential using Smoluchowski's equation.

2.4. Well water sampling

A well water sample was collected from the State of Chihuahua, Mexico.

2.5. Drinking water characterization

The parameters: Alkalinity, pH, color, electrical conductivity, acidity, chlorides, total hardness, phosphates, nitrates, nitrites, sulfates, arsenic, calcium, magnesium, potassium, sodium, and fluoride were analyzed by the standard methods and the bicarbonate content was calculated [18].

2.6. Column experiments

Fixed-bed column experiments were performed using a borosilicate glass column of 9 mm internal diameter and 20 cm length. The column was packed with aluminum modified CP. The column studies were conducted to evaluate the effect of different bed weights on the breakthrough curves. Fixed bed experiments were carried out using a solution of 3 mg/L of fluoride ions (pH 6.5) and well water containing 2.8 mg/L of fluoride ions (pH 8.1), flow rate of 2 mL/min, and 4, 6, and 8 g of CP-Al with bed depths of 7, 10, and 13.5 cm, respectively. The influent solutions were passed in down-flow mode through the bed because in this way energy is not necessary to be applied in the process; the flow rate was checked periodically during the experiments to assure uniformity of the hydraulic retention time during experiment. Aliquots of effluent were collected at time intervals and their concentrations and pH were measured, the pH values of eluted fluoride solutions were 6.4 ± 0.59 and for well water were 7.9 ± 0.16 .

2.7. Regeneration

After saturating the column with fluoride ions, a 0.1 M sodium hydroxide solution was eluted through the fixed bed of CP-Al to regenerate the adsorbent. The regeneration process was performed until the F⁻ ion concentration in the effluent was <0.1 mg/L. The pH was measured in the influent and the effluent aliquots.

2.8. Design column

A breakthrough curve obtained with the solution of interest (well water) and the adsorbent solid (CP-Al) was used to calculate the designing parameters by both the scale-up and kinetic approaches. The

calculations were done to treat 2 m³/d of well water having a concentration of 5 mg/L of fluoride ions.

3. Results and discussion

3.1. Adsorbent characterization

The main components [19] of the corrosion products determined by X-ray diffraction are magnetite, lepidocrosite, hematite, goetite, and ferrous oxide which are found in the first three layers of corrosion formed in hydraulic systems [20]. The morphology of the corrosion products are aggregates [19–21], these disperse aggregates correspond to the top surface layer of the corrosion products. The composition of the adsorbent was reported elsewhere [22] and it was as follows: carbon (6.7%), oxygen (43.0%), iron (41.2%), aluminum (5.1%), silicon (2.8%), calcium (0.5%), and sulfur (0.9%). It is important to note that the corrosion products were characterized before and after adsorption of fluoride ions in a batch system and no changes were observed [17].

3.2. Zeta potential

Adsorption from solution at the solid–aqueous electrolyte interface is affected by the interfacial electrical characteristics of the substrate, which can be assessed by electrokinetic measurements. The single most important parameter that represents the electrical nature of the oxide–aqueous electrolyte interface is the point zero charge (pzc). In the case of oxides, the pzc is given by the proton condition in solution at which the surface charge caused by H⁺ or OH[−] binding is zero. In the absence of ions adsorbed specifically, other than H⁺ and OH[−], the pzc coincides with the isoelectric point [23]. The electrokinetic behavior of the aluminum modified corrosion products in aqueous suspensions was investigated and the pzc was determined. Fig. 1 shows zeta potential–pH curve for the adsorbent and it occurs at pH of 9 in a range of −37 to 32 mV. These results indicate that the material may agglomerate and could be a good adsorbent [24].

Zeta potential results of the aluminum modified corrosion products in the presence of various fluoride concentrations are shown in Fig. 2. This figure shows that as the initial fluoride concentration increases, the zeta potential of the adsorbent shifts to higher values. This electrokinetic behavior could be related to the adsorption of free fluoride, which can exchange with surface OH groups, zeta potentials varied from −28.9 to +16.2 mV and the pzc of the adsorbent occurs at 8.5 mg/L sodium fluoride concentration. The adsorption depends on the concentration of fluoride ions,

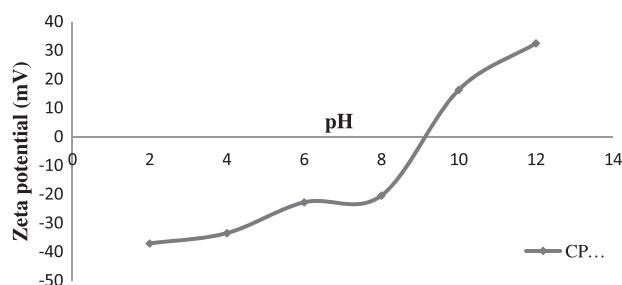


Fig. 1. pH-dependent variation of zeta potential of CP-Al.

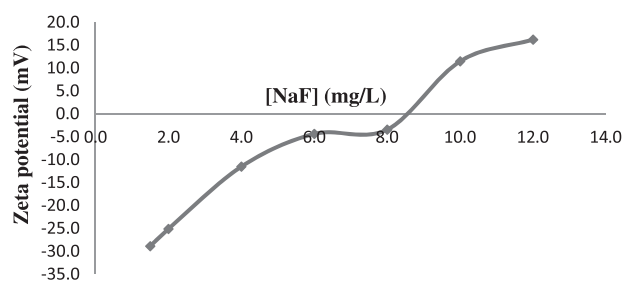


Fig. 2. Zeta potential and the variation of the ionic activity of solution.

according to the zeta potential behavior; the material presents some instability at the different fluoride concentrations which indicates that aggregates may be formed on the surface of the adsorbent [24].

3.3. Well water characterization

Table 1 shows the characterization of the well water used for the experiments, the concentration of fluoride ions is higher than the limit allowed by the World Health Organization guidelines [25]. According to Table 1, the analyzed parameters comply with the Mexican Official Standard [26] which sets the permissible limits of water for human use and consumption, with the exception of the fluoride ions. This well water has low alkalinity therefore the pH value is more susceptible to changes with time. The sodium concentration was the highest than other major cations. The anions with the highest concentration were bicarbonates and sulfates. The arsenic was found in concentrations below the permissible limit for drinking water.

3.4. Breakthrough curve

The breakthrough curve shows the loading behavior of fluoride ions removed from solution in a fixed bed and it is usually expressed in terms of adsorbed

Table 1
Characterization of well water

Parameter	Units	Value	Mexican Official Standard [26]
pH		8.05	6–8.5
Alkalinity	mg/L CaCO ₃	78.12	–
Conductivity electrical	μs/cm	425.00	–
Total hardness	mg/L CaCO ₃	110.00	500.00
Bicarbonates	mg/L	95.30	–
Sulfates	mg/L	90.00	400.00
Chlorides	mg/L	10.06	250.00
Fluorides	mg/L	2.88	1.50
N-nitrate	mg/L	0.40	10.00
Arsenic	mg/L	0.014	0.05
Calcium	mg/L	27.30	–
Magnesium	mg/L	1.79	–
Sodium	mg/L	69.84	200.00
Potassium	mg/L	2.01	–

fluoride concentration or normalized concentration defined as the ratio of effluent fluoride concentration to inlet fluoride concentration (C/C_o) as a function of time or volume of effluent for a given bed height [27]. Fig. 3 shows the breakthrough curves for fluoride adsorption using fluoride well water with different bed depths and Fig. 4 shows the comparison of the breakthrough curves for fluoride adsorption using fluoride solutions and well water at the bed depth of 7.0 cm.

Adsorbed fluoride quantity in a column for a given feed concentration and flow rate is calculated from Eq. (1) [28].

$$q_b = \frac{Q_v t_b C_o}{m_c} \quad (1)$$

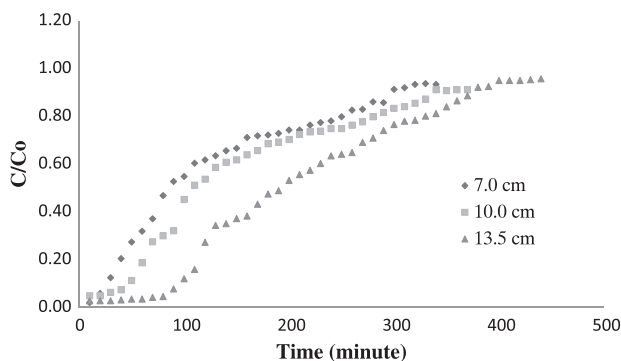


Fig. 3. Breakthrough curves of fluoride removal by aluminum modified corrosion products at different bed depths using well water.

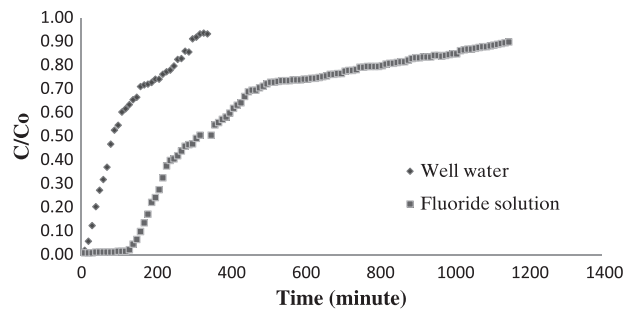


Fig. 4. Breakthrough curves of fluoride removal by aluminum modified corrosion products at bed depth of 7 cm using fluoride solution and well water.

where m_c is the mass of the adsorbent (g); C_o is the influent adsorbate concentration (mg/L); q_b is the adsorption capacity of the adsorbent at the breakthrough (mg/g); t_b is the service time (min) obtained when the concentration of the effluent reached 52% of the influent concentration which corresponds to 1.5 mg/L (permissible limit recommended by WHO) [25]; Q_v is the flow rate effluent (L/min).

The capacity values q_b and the breakthrough values at $C/C_o = 0.52$ (1.5 mg/L) are shown in Table 2, the breakthrough times increase as the columns depths increase, the adsorption capacity of the CP-Al is about four times higher for fluoride aqueous solution than well water, the composition of well water may be responsible for this behavior, the concentrations of sulfates and bicarbonate ions are higher than the concentration of other anions (chloride, nitrate, and nitrite).

Table 2
Bed depth, m_c , $t_{52\%}$, q_b for the breakthrough curves using fluoride solutions and well water

Solution	Bed depth (cm)	Bed weight m_c (g)	Breakthrough time $t_{52\%}$ (min)	Adsorbed fluoride q_b (mg/g) at breakthrough
Well water	7.0	4	88.5	0.13
	10.0	6	113.3	0.11
	13.5	8	196.0	0.14
Fluoride solution	7.0	4	352.5	0.51

3.5. Thomas model

Thomas model is used to design the maximum adsorption capacity of an adsorbent, it assumes that film diffusion resistance predominates, and neglects axial dispersion. The linearized form of Thomas model can be expressed as follows.

$$\ln\left[\frac{C_o}{C} - 1\right] = \frac{K_T q_T M}{Q} - K_T C_o t \quad (2)$$

where K_T is the Thomas model constant (L/mg min), q_T is the adsorption capacity (mg/g), Q is the volumetric flow rate through column, which was 1 mL/min, M is the mass of adsorbent in the column (g), C_o is the initial fluoride concentration (mg/L), and C is the effluent fluoride concentration (mg/L) at any time t (min). The Thomas model constants k_T and q_T were determined from a plot of $\ln [C_o/C - 1]$ vs. t at a given flow rate.

The experimental results were adjusted to this model using fluoride solutions and well water and the parameters determined for the breakthrough curves are given in Table 3. The Thomas model constant increased as the bed depth increased and the adsorption for well water was lower than fluoride solution, this behavior was similar to the results reported by García-Sánchez et al. [17].

3.6. Adams–Bohart model

The Adams–Bohart model is used for the description of the initial part of a breakthrough curve. This model provides a simple and comprehensive approach to evaluate sorption column test, but its validity is limited in the concentration $C < 0.5C_o$ range [29]. The linear form of Adams–Bohart model can be expressed as follows.

$$\ln\left(\frac{C}{C_o}\right) = K_{AB} C_o t - K_{AB} N_o \frac{Z}{V} \quad (3)$$

where K_{AB} is the kinetic constant (L/mg min), V is the linear flow rate (cm/min), Z is the bed depth of column (cm), and N_o is the saturation concentration (mg/L). The linear flow rate was calculated from the equation $V = Q/A$, where Q = volumetric flow (mL/min) and A is the transversal area of the column (cm²). The Adams–Bohart model constants K_{AB} and N_o were determined from a plot of $\ln (C/C_o)$ vs. t .

This approach was focused on breakthrough, relative values of K_{AB} and N_o were calculated using linear regression analysis and they are presented in Table 3, and the values of R^2 were between 0.89 and 0.96. In general, the values of K_{AB} decreased as the bed depth increased from 7.0 to 13.5 cm.

Table 3
Thomas and Adams–Bohart models parameters for the breakthrough curves using fluoride solutions and well water

Solution	Bed depth (cm)	Thomas model			Adams–Bohart model (50%)		
		k_T (mL/mg min)	q_o (mg/g)	R^2	K_{AB} (mL/mg min)	N_o (mg/L)	R^2
Well water	7.0	3.90	0.15	0.9449	9.86	110.06	0.8990
	10.0	4.62	0.15	0.8871	9.17	95.47	0.9671
	13.5	5.49	0.16	0.9599	6.90	113.90	0.9338
Fluoride solution	7.0	0.83	0.34	0.9384	5.76	332.04	0.9248

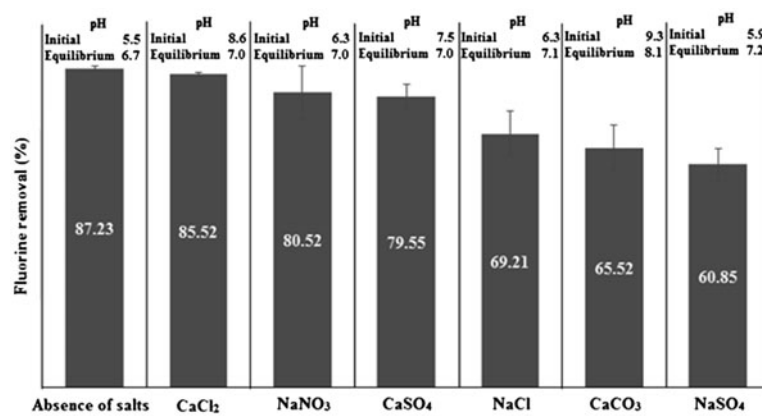


Fig. 5. Effects of anions on the adsorption of fluoride ions from solutions by CP-Al.

3.7. Assessment of influence of interfering co-ions

Defluoridation performance of CP-Al were carried out in the presence of common ions (CaCl₂, NaNO₃, CaSO₄, NaCl, CaCO₃, Na₂SO₄), which are normally present in well water. The concentration of co-existing ions was 0.1 M with an initial fluoride concentration of 5 mg/L (Fig. 5). The equilibrium pH values in these solutions were from 5.5 to 9.3, it is important to note that the presence of hydroxyl anions affects the adsorption of fluoride. As shown in Fig. 5, the effects of the anions on the adsorption of fluoride ion decreases as follows: Cl⁻ (CaCl₂) > NO₃⁻ (NaNO₃) > SO₄²⁻ (CaSO₄) > Cl⁻ (NaCl) > CO₃²⁻ (CaCO₃) > SO₄²⁻ (Na₂SO₄), as it can be observed, the anions and cations play an important role on the adsorption of fluoride ions. Martínez et al. [19] found that the adsorption efficiency of unmodified oxides for the adsorption of fluoride was affected by the presence of anions in the following way: Bicarbonate > fluoride > chloride > > > sulfate ≈ nitrate. It is not possible to compare these results because the effects depend on the anions and cations present in the solution, and the presence of the high concentrations of sodium and sulfate affect, in an important way, the adsorption of fluoride ions.

3.8. Regeneration

In order to regenerate the adsorbent, a 0.1 M sodium hydroxide solution was eluted through the column with a flow rate of 2 mL/min after it was saturated with fluoride ions. The regeneration curve is shown in Fig. 6, as it can be observed, the fluoride ions could be eluted with about 150 mL of sodium hydroxide solution. Unfortunately, the material after regeneration showed a very poor adsorption of fluoride ions, only 3.5%.

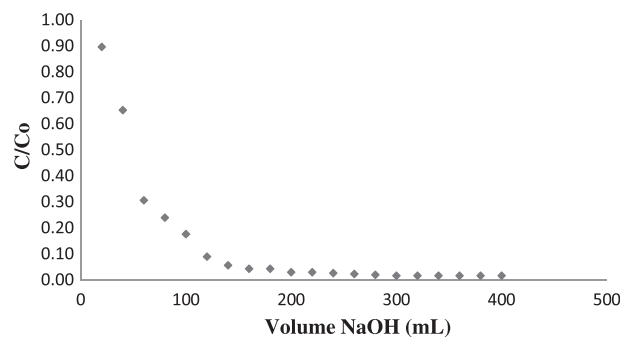


Fig. 6. Elution of fluoride during regeneration.

3.9. Design and scale-up

3.9.1. Scale-up approach

The principle experimental information required for calculations is a breakthrough curve from a test column, either laboratory or pilot scale, that has been operated at the same liquid flow rate in terms of bed volumes per unit time, Q_b , as the design column. Since the contact times are the same, it is assumed that the volume of liquid treated per unit mass of adsorbent, V_B , for a given breakthrough in the test column is the same as for the design column. Before a breakthrough test can be performed, it is necessary to select a satisfactory liquid flowrate, Q_b , in bed volumes per unit time. This may be estimated from calculations using the required breakthrough volume, the solute concentration, the maximum solid-phase concentration, and other pertinent data [30].

The bed volume of the design column is given by:

$$\text{Bed volume (BV)} = \frac{Q}{Q_b} \quad (4)$$

where Q is the design liquid flowrate. The mass or weight of the adsorbent, M , for the design column is determined from:

$$M = (BV)(\varphi_S) \tag{5}$$

where φ_S is the adsorbent bulk density. From the breakthrough curve of the laboratory column, the breakthrough volume, V_B , is determined for the allowable effluent solute concentration, C_a . The volume of liquid treated per unit mass of adsorbent, \tilde{V}_B , is then determined by,

$$\tilde{V}_B = V_B/M \tag{6}$$

where M is the mass of the adsorbent in the test column. The mass of adsorbent exhausted per hour, M_t , for the design column is computed from:

$$M_t = Q/\tilde{V}_B \tag{7}$$

where Q is the design liquid flowrate. The breakthrough time, T , is,

$$T = \frac{M}{M_t} \tag{8}$$

where M is the mass of adsorbent in the design column. The calculated breakthrough volume, V_B , for the allowable breakthrough concentration, C_a , for the design column is,

$$V_B = QT \tag{9}$$

It is important to note that in scale-up model, T and Q/A are the same for laboratory column and the design column.

3.9.2. Kinetic approach

This method utilizes a kinetic equation based on the derivation by Thomas. The principle experimental information required is a breakthrough curve from a test column [30].

The expression by Thomas for an adsorption column is as follows:

$$\frac{C}{C_o} = \frac{1}{1 + e^{\frac{K_T}{Q}(q_o M - C_o V)}} \tag{10}$$

where C is the effluent solute concentration (mg/L), C_o is the influent solute concentration (mg/L), K_T is the rate constant (L/mg min), q_T is the maximum solid-phase concentration of the sorbed solute (kg/kg), M is the mass of the adsorbent (kg), V is the through-put volume (L), Q is the volumetric flow rate through column (L/h).

Assuming that the left side equals the right side, cross multiplying gives,

$$1 + e^{\frac{K_T}{Q}(q_o M - C_o V)} = \frac{C_o}{C} \tag{11}$$

Rearranging and taking the natural logarithms on both sides, yields the design equation,

$$\ln \left[\frac{C_o}{C} - 1 \right] = \frac{K_T q_T M}{Q} - \frac{K_T C_o}{Q} V \tag{12}$$

From Eq. (12), it can be seen that this is a straight-line. The terms are $y = \ln (C_o/C - 1)$, $x = V$, $m = K_T C_o/Q$, and $b = K_T q_T M/Q$.

Table 4 shows the parameters calculated by both methods to treat 2 m³ of water per day; the breakthroughs were reached with 128 L considering the breakthrough curves obtained in the laboratory with 7 cm of bed heights. The models gave similar results, although the required mass to treat the same volume of water is higher for the scale-up model than kinetic

Table 4
Parameters derived from the analysis of the design equations

	Result C1
<i>Scale-up model</i>	
Adsorbent mass (M)	2.84 kg
Bed volume per unit time (Q_b)	22 BV/h
Mass of adsorbent exhausted per hour (M_t)	1.85 kg/h
Breakthrough time (t_B)	1.54 h
Breakthrough volume (V_B)	128 L
Column diameter (d)	26 cm
Bed height (H_b)	7.0 cm
Column height (H_c)	130 cm
<i>Kinetic model</i>	
Thomas rate constant (K_T)	0.037 L/s kg
Adsorption capacity (q_T)	0.26 kg/kg
Adsorbent mass (M)	2.0 kg
Column diameter (d)	26.0 cm
Bed height (H_b)	5.0 cm
Column height (H_c)	130 cm

model, similar behavior was observed by Reynolds and Richards [30].

4. Conclusions

The experimental results were fitted to the Bohart–Adams and Thomas models; the adsorption efficiency decreases as the bed depth increases. The adsorption capacity for fluoride ions by CP-Al is higher for fluoride aqueous solutions than well water; this behavior could be attributed to the composition of the well water, mainly due to the presence of high concentrations of the sodium and sulfate ions. The effects of the anions on the adsorption of fluoride ion decreased as follows: $\text{Cl}^- (\text{CaCl}_2) > \text{NO}_3^- (\text{NaNO}_3) > \text{SO}_4^{2-} (\text{CaSO}_4) > \text{Cl}^- (\text{NaCl}) > \text{CO}_3^{2-} (\text{CaCO}_3) > \text{SO}_4^{2-} (\text{Na}_2\text{SO}_4)$. The regeneration of the material was accomplished with NaOH solution but only a little removal of fluoride ions in the second adsorption cycle was observed. Scale-up and kinetic approach methods were used to calculate the design parameters from the breakthrough curves of fixed-bed column experiments to treat 2 m^3 of well water containing 5 mg/L of fluoride ions.

Acknowledgments

We acknowledge financial support from CONACYT, project 131174Q, and scholarship grant number 209761 for JJGS.

References

- [1] M.G. McGrady, R.P. Ellwood, P. Srisilapanan, N. Korwanich, H.V. Worthington, I.A. Pretty, Dental fluorosis in populations from Chiang Mai, Thailand with different fluoride exposures—Paper 1: Assessing fluorosis risk, predictors of fluorosis and the potential role of food preparation, *BMC Oral Health*. 12 (2012) 16–28.
- [2] S. Ghorai, K.K. Pant, Investigations on the column performance of fluoride adsorption by activated alumina in a fixed-bed, *Chem. Eng. J.* 98 (2004) 165–173.
- [3] A.A.M. Daifullah, S.M. Yakout, S.A. Elreefy, Adsorption of fluoride in aqueous solutions using KMnO_4 -modified activated carbon derived from steam pyrolysis of rice straw, *J. Hazard. Mater.* 147 (2007) 633–643.
- [4] K. Vaaramaa, J. Lehto, Removal of metals and anions from drinking water by ion exchange, *Desalination* 155 (2003) 157–170.
- [5] S. Saha, Treatment of aqueous effluent for fluoride removal, *Water Res.* 27 (1993) 1347–1350.
- [6] P.I. Ndiaye, P. Moulin, L. Dominguez, J.C. Millet, F. Charbit, Removal of fluoride from electronic industrial effluent by RO membrane separation, *Desalination* 173 (2005) 25–32.
- [7] Z. Amor, B. Bariou, N. Mameri, M. Taky, S. Nicolas, A. Elmidaoui, Fluoride removal from brackish water by electrodialysis, *Desalination* 133 (2001) 215–223.
- [8] M. Mahramanlioglu, I. Kizilcikli, I.O. Bicer, Adsorption of fluoride from aqueous solution by acid treated spent bleaching earth, *J. Fluorine Chem.* 115 (2002) 41–47.
- [9] A.M. Raichur, M.J. Basu, Adsorption of fluoride onto mixed rare earth oxides, *Sep. Purif. Technol.* 24 (2001) 121–127.
- [10] G. Moges, F. Zewge, M. Socher, Preliminary investigations on the defluoridation of water using fired clay chips, *J. Afr. Earth Sci.* 22 (1996) 479–482.
- [11] Y. Wang, E.J. Reardon, Activation and regeneration of a soil sorbent for defluoridation of drinking water, *Appl. Geochem.* 16 (2001) 531–539.
- [12] D.S. Bhargava, D.J. Killedar, Fluoride adsorption on fishbone charcoal through a moving media adsorber, *Water Res.* 26 (1992) 781–788.
- [13] M.S. Onyango, Y. Kojima, A. Kumar, D. Kuchar, M. Kubota, H. Matsuda, Uptake of fluoride by Al^{3+} -pretreated low-silica synthetic zeolites: Adsorption equilibrium and rate studies, *Sep. Sci. Technol.* 41 (2006) 683–704.
- [14] E. Kumar, A. Bhatnagar, M. Ji, W. Jung, S. Lee, S.J. Kim, G. Lee, H. Song, J.Y. Choi, J. Yang, B.H. Jeon, Defluoridation from aqueous solutions by granular ferric hydroxide (GFH), *Water Res.* 43 (2009) 490–498.
- [15] S.V. Mohan, S.V. Ramanaiah, B. Rajkumar, P.N. Sarma, Removal of fluoride from aqueous phase by biosorption onto algal biosorbent *Spirogyra* sp-IO2: sorption mechanism elucidation, *J. Hazard. Mater.* 141 (2007) 465–474.
- [16] S. Ayoob, A.K. Gupta, V.T. Bhat, A conceptual overview on sustainable technologies for defluoridation of drinking water, *Crit. Rev. Env. Sci. Technol.* 38 (2008) 401–470.
- [17] J.J. García-Sánchez, M. Solache-Ríos, V. Martínez-Miranda, C. Solís Morelos, Removal of fluoride ions from drinking water and fluoride solutions by aluminum modified iron oxides in a column system, *J. Colloid Interface Sci.* 407 (2013) 410–415.
- [18] W.J. Deutsch, *Groundwater Geochemistry Fundamentals and Applications To Contamination*, first ed., CRC Press LLC, Washington, DC, 1997.
- [19] V. Martínez-Miranda, J.J. García-Sánchez, M. Solache-Ríos, Fluoride ions behavior in the presence of corrosion products of iron: Effects of other anions, *Sep. Sci. Technol.* 46 (2011) 1443–1449.
- [20] P.V.L. Sarin, L.D.A. Snoeyink, W.M. Kriven, Iron corrosion scales: Model for scale growth, iron release and colored water formation, *J. Environ. Eng.* 130 (2004) 364–373.
- [21] H.M. Herro, R.D. Port, *The Nalco Guide to Cooling Water System, Failure Analysis*, McGraw-Hill, New York, NY, 1993.
- [22] J.J. García-Sánchez, V. Martínez-Miranda, M. Solache-Ríos, Aluminum and calcium effects on the adsorption of fluoride ions by corrosion products, *J. Fluorine Chem.* 145 (2013) 136–140.
- [23] J.L. Reyes-Bahena, A. Robledo-Cabrera, A. López-Valdivieso, R. Herrera-Urbina, Fluoride adsorption onto $\alpha\text{-Al}_2\text{O}_3$ and its effect on the zeta potential at the alumina-aqueous electrolyte interface, *Sep. Sci. Technol.* 37 (2002) 1973–1987.
- [24] J. Kim, D.F. Lawler, Characteristics of zeta potential distribution in silica particles, *Bull. Korean Chem. Soc.* 26 (2005) 1083–1089.

- [25] World Health Organization, Guidelines for Drinking-water Quality, fourth ed., 2012, pp. 370–373. Available from: http://whqlibdoc.who.int/publications/2011/9789241548151_eng.pdf.
- [26] NOM-127-SSA1-2000, Modificación de la Norma Oficial Mexicana NOM-127-SSA1-(1994) Salud ambiental Agua para uso y consumo humano Límites permisibles de calidad y tratamientos a que debe someterse el agua para su potabilización (Modification of the Mexican official regulation NOM-127-SSA1-(1994) Environmental health. Water for human consumption and use. Permissible limits of quality and water treatments for its purification).
- [27] Z. Aksu, F. Gönen, Bio sorption of phenol immobilized activated sludge in a continuous packed bed: Prediction of breakthrough curves, *Process Biochem.* 39 (2004) 599–613.
- [28] V.C. Taty-Costodes, H. Fauduet, C. Porte, Y.S. Ho, Removal of lead (II) ions from synthetic and real effluents using immobilized *Pinus sylvestris* sawdust: Adsorption on a fixed-bed column, *J. Hazard. Mater.* 123 (2005) 135–144.
- [29] R. Han, L. Zou, X. Zhao, Y. Xu, F. Xu, Y. Li, Y. Wang, Characterization and properties of iron oxide-coated zeolite as adsorbent for removal of copper (II) from solution in fixed bed column, *Chem. Eng. J.* 149 (2009) 123–131.
- [30] T.D. Reynolds, P. Richards, *Unit Operations and Processes in Environmental Engineering*, second ed., Cengage Learning, Boston, MA, 1996, pp. 350–373.